EARTH SURFACE PROCESSES AND LANDFORMS
Earth Surf. Process. Landforms **40**, 1542–1559 (2015)

Published online 23 June 2015 in Wiley Online Library
(wileyonlinelibrary.com) DOI: 10.1002/esp.3755

Hydro-meteorological drivers and sources of suspended sediment flux in the pro-glacial zone of the retreating Castle Creek Glacier, Cariboo Mountains, British Columbia, Canada

Michael S. Leggat,[1] Philip N. Owens,[1]* Tim A. Stott,[2] Barry J. Forrester,[2] Stephen J. Déry[1] and Brian Menounos[3]
[1] Environmental Science Program and Quesnel River Research Centre, University of Northern British Columbia, Prince George, British Columbia, Canada
[2] Faculty of Education, Health & Community, Liverpool John Moores University, Liverpool, UK
[3] Natural Resources and Environmental Studies Institute and Geography Program, University of Northern British Columbia, Prince George, British Columbia, Canada

Received 30 September 2013; Revised 26 March 2015; Accepted 11 May 2015

*Correspondence to: Philip N. Owens, Environmental Science Program and Quesnel River Research Centre, University of Northern British Columbia, Prince George, British Columbia, V2N 4Z9, Canada. E-mail: philip.owens@unbc.ca

ESPL
Earth Surface Processes and Landforms

ABSTRACT: Glaciers are major agents of erosion that increase sediment load to the downstream fluvial system. The Castle Creek Glacier, British Columbia, Canada, has retreated ~1.0 km in the past 70 years. Suspended sediment concentration (SSC) and streamflow (*Q*) were monitored independently at five sites within its pro-glacial zone over a 60 day period from July to September 2011, representing part of the ablation season. Meteorological data were collected from two automatic weather stations proximal to the glacier. The time-series were divided into hydrologic days and the shape and magnitude of the SSC response to hydro-meteorological conditions ('cold and wet', 'hot and dry', 'warm and damp', and 'storm') were categorized using principal component analysis (PCA) and cluster analysis (CA). Suspended sediment load (SSL) was computed and summarized for the categories. The distribution of monitoring sites and results of the multivariate statistical analyses describe the temporal and spatial variability of suspended sediment flux and the relative importance of glacial and para-glacial sediment sources in the pro-glacial zone. During the 2011 study period, ~ 60% of the total SSL was derived from the glacial stream and sediment deposits proximal to the terminus of the glacier; during 'storm' events, that contribution dropped to ~40% as the contribution from diffuse and point sources of sediment throughout the pro-glacial zone and within the meltwater channels increased. While 'storm' events accounted for just 3% of the study period, SSL was ~600% higher than the average over the monitoring period, and ~20% of the total SSL was generated in that time. Determining how hydro-meteorological conditions and sediment sources control sediment fluxes will assist attempts to predict how pro-glacial zones respond to future climate changes. Copyright © 2015 John Wiley & Sons, Ltd.

KEYWORDS: suspended sediment; pro-glacial; British Columbia; sediment budget; turbidity; para-glacial sediment sources

Introduction

Glaciers in British Columbia (BC), Canada, cover about 3% (~29 000 km^2) of the landmass (Moore *et al.*, 2009), and all lost substantial mass in response to regional climate warming of 0.5 to 1.5 °C per century since the end of the Little Ice Age (Schiefer *et al.*, 2007; Bolch *et al.*, 2010; Tennant *et al.*, 2012). Although current global climate models do not explicitly include glacial evolution (Syvitski and Milliman, 2007), it is expected that glaciers will continue to retreat in response to the projected 1 to 4 °C increase in global mean surface temperature, depending on the emission scenario, over the next 100 years (Collins *et al.*, 2013).

Changes in meteorological conditions and glacial retreat have been linked to increased variability of streamflow in recent decades, specifically the quantity and quality (i.e. temperature, sediment load, chemistry) of water and hydrograph timing (Déry *et al.*, 2012; Kirtman *et al.*, 2013). Consequently, there is much concern associated with the potential impacts of climate change, including glacial retreat, on river flows and sediment fluxes in BC [Fraser Basin Council (FBC), 2008; Moore *et al.*, 2009; Déry *et al.*, 2012].

Glacier retreat exposes unconsolidated sediments that are vulnerable to rapid and extensive erosion and entrainment into the fluvial system (Ballantyne, 2002). These pro-glacial sediment sources tend to be spatially and temporally variable and transient, depending on site specific characteristics (Gurnell *et al.*, 1996; Ballantyne, 2002; Tunnicliffe and Church, 2011). Immediately after exposure, the unconsolidated and water-saturated diamicton in the pro-glacial zone begins to adjust to subaerial conditions; loose sediments consolidate as the substrate drains, and slope angles decline (Ballantyne, 2002). Over time, the eluviation of fines, surface armouring, reduction in surface slope and vegetation colonization act to stabilize the pro-glacial zone and reduce sediment availability for fluvial entrainment and transport (Warburton, 1990; Gurnell *et al.*, 1999; Orwin and Smart, 2004). Church and Ryder (1972) reported that erosion of glacial deposits in a pro-glacial or post-glacial fluvial environment results in heightened sediment transport that continues as long as the sediment remains easily accessible for fluvial erosion and transportation.

The pro-glacial zone can function as a significant source or sink of sediment, which can vary over a single ablation season (Hammer and Smith, 1983; Warburton, 1990; Hodson *et al.*, 1998; Orwin and Smart, 2004; Cockburn and Lamoureux, 2008; Stott *et al.*, 2008), over the seasons of a year (Richards and Moore, 2003), from year to year (Hodgkins *et al.*, 2003; Stott and Mount, 2007), over the para-glacial period due to 'glacially conditioned sediment release' (Church and Ryder, 1972; Ballantyne, 2002), and over longer periods as glaciers expand and contract in response to broader climatic trends (Church and Slaymaker, 1989; Moore *et al.*, 2009). Abnormally warm ablation seasons have been shown to increase sediment yield from the pro-glacial zone (Stott and Mount, 2007), whereas, cooler seasons have been found to increase sediment storage (Hodgkins *et al.*, 2003; Richards and Moore, 2003).

Sediment sources in the pro-glacial zone also vary in response to site and meteorological conditions. Warburton (1990) found that 77% of the sediment output from the Bas Glacier d'Arolla in Switzerland was derived from the glacier and snout zone moraine deposits and that channel processes were primarily responsible for modifying sediment loads within the pro-glacial zone. Orwin and Smart (2004) conducted an intensive study of suspended sediment fluxes in the pro-glacial zone of the Small River Glacier, BC (located only ~50 km from the site of the present study), and found that the pro-glacial area was the source for up to 80% of the total suspended sediment yield (SSY) transferred from the basin during part of the 2000 ablation season. Furthermore, sub-glacial sediment sources can be an important (Warburton, 1990; Swift *et al.*, 2002; Haritashya *et al.*, 2010) or not so important (Hammer and Smith, 1983; Orwin and Smart, 2004) component of the pro-glacial suspended sediment budget, and this depends on the slope of the pro-glacial zone and other site specific geologic, glacial and pro-glacial characteristics (Gurnell *et al.*, 1996; Schiefer *et al.*, 2001), as well as weather and climate patterns during the study (Richards and Moore, 2003; Moore *et al.*, 2009).

Given the diversity of findings in terms of the response of pro-glacial zones to hydro-meteorological drivers and sediment sources, a better understanding of the processes of sediment exchange in pro-glacial zones and the effect of meteorological conditions on those processes could improve predictive modelling of river sediment dynamics and, thereby, the effect on downstream aquatic ecosystems and water resources (Milner *et al.*, 2009; Moore *et al.*, 2009; Owen *et al.*, 2009). The anticipated changes in climate (i.e. temperature and precipitation) and the complexity associated with such changes [Intergovernmental Panel on Climate Change (IPCC), 2013] make it important to understand how fine-grained sediment fluxes from glacial and para-glacial sources could respond (Moore *et al.*, 2009).

The focus of this study is on the flux of fluvial suspended sediment < 2 mm through the pro-glacial zone and the influence of hydro-meteorological conditions. We monitored streamflow (*Q*) and suspended sediment concentration (SSC) in the pro-glacial meltwater channels of the Castle Creek Glacier, BC, during part of the snow-free period in summer 2011 and obtained meteorological data from proximal weather stations to: (i) examine the spatial and temporal response pattern of SSC; and, (ii) determine the sources of *Q* and suspended sediment load (SSL) under different hydro-meteorological conditions. We hypothesize that: (i) short-term suspended sediment fluxes within the pro-glacial zone respond to hydro-meteorological conditions; and (ii) exposed sediment adjacent to the glacier snout contributes substantially to downstream sediment yield.

Study Area and Methods

Study area

Castle Creek Glacier (CCG) (53°2′ N, 120°24′ W, unofficial name), has an area of ~9 km^2, a length of ~6 km, an elevation range of 1870 to 2850 m above sea level (a.s.l.) and is located in the Cariboo Mountains of eastern BC, ~180 km southeast of Prince George (Figure 1, Beedle *et al.*, 2009). Beedle *et al.* (2009) used a series of annual push moraines and aerial photographs to determine that the glacier retreated 886 m between 1946 and 2007, an average of 14 m a^{-1} (Figure 1). After flowing through a small gorge and leaving the recently exposed pro-glacial zone, meltwater draining from CCG flows generally northeast for ~34 km before flowing into the upper Fraser River, which drains into the Pacific Ocean at Vancouver, BC, after a distance of ~1375 km.

The scope of this study was on the meltwater channels and sediment sources in the pro-glacial area from the snout of the glacier 1870 m a.s.l. to the small gorge 1790 m a.s.l. The catchment area above the gorge was ~16 km^2 and was ~60% glacierized in 2011 (Table I), stream distance was ~1.2 km with an average slope of ~3% (Figure 2). The area immediately downslope from the snout of the glacier was characterized by low relief till sheets, outwash fans, abandoned meltwater channels, and bedrock outcrops. The till deposits on the west side of the meltwater channel have been substantially eroded and modified by several abandoned meltwater channels incised to varying depths (up to 5 m) which end at abandoned outwash fans. The east side of the meltwater channel was characterized by two relatively intact till sheets separated by an outwash fan complex (Figure 1). Most of the pro-glacial zone is devoid of vegetation such that sediment is exposed to weathering and erosion. Three streams flow from the receding snout of CCG: (1) a small ice-marginal meltwater stream drains the east side of the glacier; (2) the main flow emanates from a sub-glacial channel portal on the northwest side of the glacier's snout; and (3) a small stream drains a pro-glacial lake perched on a till sheet that extends out from the terminus of the glacier drains northwest over bedrock into the main channel (Figure 1).

Methods

Streamflow and SSC were monitored for 60 days between 13 July and 11 September 2011 (Julian Day (JD) 195–JD 254) at five stations (Figure 1): three proximal sites (PS1, PS2 and PS3) on the meltwater streams from the glacier (1870 m a.s.l.); a middle site (MS) below the confluence of the three streams (~0.65 km from the glacier snout and 1800 m a.s.l); and a distal site (DS) at the bedrock gorge (~1.2 km from the glacier snout and 1790 m a.s.l.). The majority of the seasonal snowpack had already melted from the pro-glacial area prior to the start of data collection and thus the monitoring period does not represent the full ablation period.

Meteorological data were collected from two automatic weather stations (AWSs): one located on a bedrock ridge on the south side of CCG at 2105 m a.s.l.; the other was located

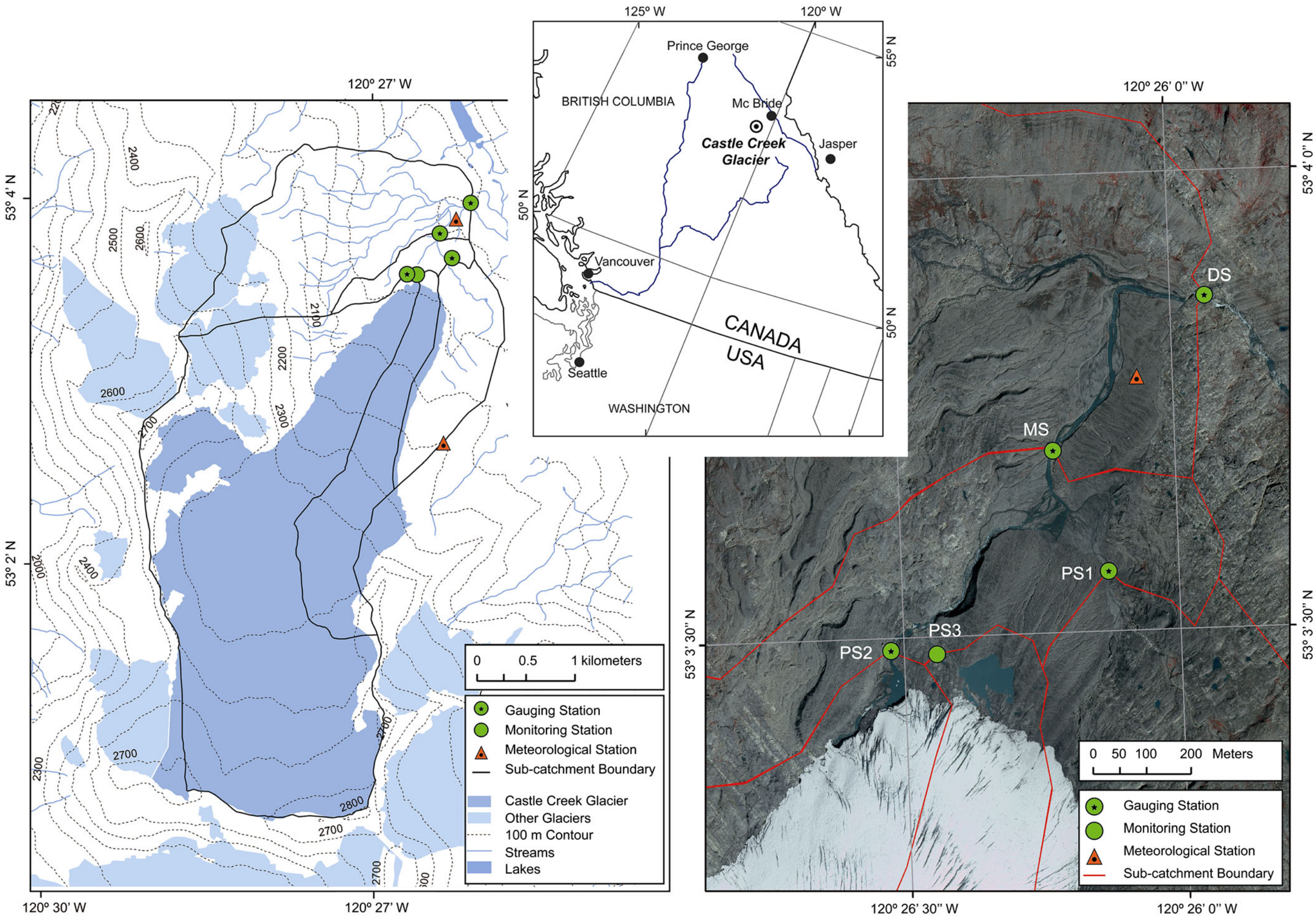

Figure 1. Location of Castle Creek Glacier (inset) and pro-glacial zone of the Castle Creek Glacier with the 2011 sampling locations, approximate watershed boundaries and the meteorological stations. Turbidity and suspended sediment data were collected at monitoring stations, water level and streamflow data were additional parameters collected at the gauging stations. This figure is available in colour online at wileyonlinelibrary.com/journal/espl

Table I. Catchment areas and percentage glacial cover for pro-glacial stream monitoring sites

Site	Total area (km^2)	Glacierized (km^2)	Un-glacierized (km^2)	Percentage glacierized (%)
Castle Creek Glacier	8.96	8.96	0.00	100
PS1	1.24E[a]	0.14E	1.10	11
PS2	9.36E	7.19E	2.17	77
PS3	1.73E	1.64E	0.09	95
MS	12.69	8.96	3.73	71
DS	15.68	9.46	6.22	60

[a]E, estimated.

on the low gradient till apron near MS, at ~1800 m a.s.l. (Figure 1). These stations are part of the Cariboo Alpine Mesonet operated by the University of Northern British Columbia (UNBC; Déry *et al.*, 2010). The parameters measured every 15 minutes by the AWSs include wind speed and direction, snow height, liquid precipitation (rainfall equivalent), air temperature, incoming solar radiation, relative humidity and atmospheric pressure. These meteorological parameters relate to snow and glacial ice accumulation and melt, and surface runoff, and thus determine the temporal and spatial pattern of streamflow and sediment flux processes.

Streamflow (*Q*) was gauged at four sites (PS1, PS2, MS and DS) that were equipped with water level monitoring equipment. Hobo U20 pressure transducers (Onset Computer Corp., Bourne, MA, USA; resolution ± 4.5 mm) were fixed vertically in stilling wells and surveyed to local benchmarks to maintain vertical control throughout the study period. Barometric pressure from the lower AWS was used to correct the absolute pressure record from the pressure transducers to isolate pressure change due to water level. Stream gauging was conducted with an OTT-type (Ott, Kempten, Germany) horizontal impeller meter on a wading rod following the mid-section method [Resource Inventory Standards Committee (RISC), 2009]. With the exception of one site (PS1), eight discharge measurements distributed over the wadeable range of *Q* were used to develop stage-discharge rating curves (Table II). The main channel was not safe to wade above 5 $m^3 s^{-1}$ and rating curve extensions were used to compute *Q* data above this level. Rating curve extensions are considered valid up to two times the maximum gauged flow and an estimate thereafter [Water Survey of Canada (WSC), 2012]. In the worst case, 0.6% of the *Q* record at DS was considered an estimate. The five minute interval *Q*

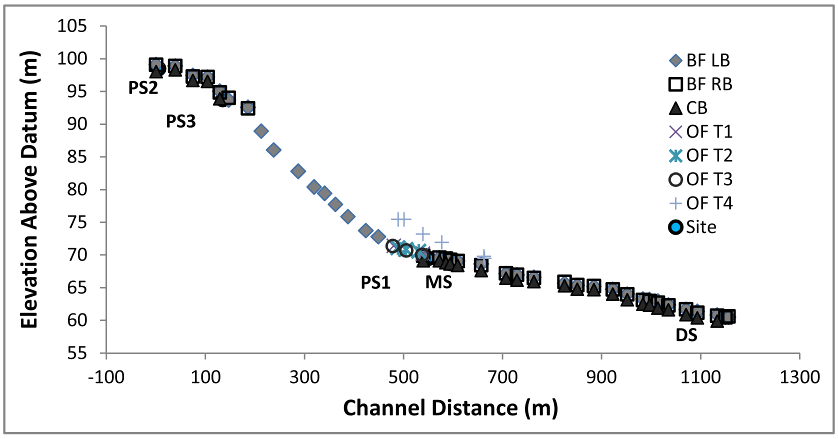

Figure 2. Longitudinal stream profile for Castle Creek pro-glacial meltwater channel: BF LB, bankfull left bank; BF RB, bankfull right bank; CB, channel bottom; OF T1 though T4, outwash fan transects 1 through 4. Datum was arbitrarily set 100 m below the highest benchmark, and zero channel distance was set as the outflow of the pro-glacial lake upstream of site PS2 (Figure 1). This figure is available in colour online at wileyonlinelibrary.com/journal/espl

Table II. Summary data of regressions of (a) water level (WL, m) against streamflow (Q, $m^3 s^{-1}$), based on river gauging, and (b) suspended sediment concentration (SSC, mg l^{-1}) against turbidity (Tu, NTU)[a]

	Site	N	Normally distributed	Regression equation	R^2 Value	95% Confidence interval
(a)	PS1	4	—	$Q = 325.002 \times WL6.58$	—	—
	PS2	8	—	$Q = 13.125 \times WL2.056$	—	—
	MS	8	—	$Q = 18.864 \times WL1.873$	—	—
	DS	8		$Q = 27.321 \times WL1.946$	—	—
(b)	PS1	18	Y	SSC = 304.59 × Tu − 54.19	0.43	57.6
	PS2	156	Y	SSC = 252.53 × Tu + 8.63	0.79	2.8
	PS3	82	Y	SSC = 180.45 × Tu − 23.60	0.85	9.1
	MS	176	Y	SSC = 213.80 × Tu + 8.05	0.67	3.6
	DS	169	Y	SSC = 413.04 × Tu − 23.26	0.77	5.4

[a]For plots see on-line Supplementary Material.

record for PS3 was deduced as the difference between the downstream record at MS and the sum of PS2 and PS1 records. This deductive method assumes that there is no other flow entering or leaving the channel within the reach, which would be false under certain conditions (i.e. snowmelt or intense precipitation) and thus Q and SSL at PS3 may have a larger margin of error.

Suspended sediment concentration was monitored at all five sites. During site selection, a DH 48 depth integrating suspended sediment sampler was used to confirm that the stream was well mixed and that the sample point was representative, as would be expected due to the turbulent nature of the flow (Gurnell *et al*., 1992, Navratil *et al*., 2011). Analite 195 turbidity probes (McVan Instruments Pty Ltd, Mulgrave, Australia) were installed on a floating apparatus with a water intake for the Teledyne Isco 6700 automatic samplers (Teledyne Isco, Inc., Lincoln, NB, USA). The sample interval and strategy varied from discrete 800 ml samples every two, three, four or six hours to daily composite samples based on the capacity of the field team to process samples. Discrete water samples were measured with a graduated cylinder, vacuum filtered in the field through pre-dried and pre-weighed Whatman GF/D ashless 8 μm filter papers, labelled, stored, and brought back to the UNBC Landscape Ecology laboratory for gravimetric analysis of SSC. The use of 8 μm filter papers was based on the need to process hundreds of filter papers in the field. It is possible that this resulted in the loss of fine sediment < 8 μm. However, the use of 8 μm filter papers is common in similar studies in pro-glacial environments (e.g. Hodgkins 1999; Orwin and Smart, 2004), and Gurnell *et al*. (1992) demonstrated that such filter papers retain most of the < 8 μm fraction due to clogging of pores. We assessed the representativeness of 8 μm filter papers by filtering paired samples collected over a range of SSC at the five study sites, in which one sample was filtered in the field using 8 μm filter papers and the second was filtered in the laboratory using 0.45 μm cellulose nitrate membrane filters. The average difference was < 8% (there was no significant difference between the sites), which is consistent with the findings of others (e.g. Gurnell *et al*., 1992) and thus we believe the use of 8 μm filter papers has a limited influence on estimates of suspended sediment loads and fluxes.

The SSC samples were paired with the synchronous turbidity (Tu) value for the site. The fourth spread method (Jacobs and Dinman, 2013) was used as a quantitative method to remove outliers in the paired data. A probability plot correlation coefficient (PPCC) was computed for each data set and the critical value (CV) at the 5% significance level was obtained for the given sample size from a PPCC CV table (Filliben and Devaney, 2013). The null hypothesis that the data came from a population with a normal distribution cannot be rejected when the PPCC is greater than the CV (Filliben and Devaney, 2013). Linear regression equations were generated for each data set to compute SSC from the five minute Tu record (Table II).

Two of the sites, PS1 and PS3, had data that exceeded the range of the Tu meter. These data were left in the analysis as a better option than deleting or fabricating values. The 95% confidence intervals show that there was greater uncertainty with the PS1 and PS3 regressions (Table II). PS1 was a small stream and the duration of exceedances decreased through the field season. The exceedances at PS3 occurred during periods of low flow, and were partially removed as erroneous data due to the sample intake point being too close to the streambed. Due to low flow volume, the effect of the exceedances on the SSL results at PS1 and PS3 was limited.

The pressure transducers and Tu data loggers were programmed to observe water level and Tu every minute and to log an average value every five minutes. During the analysis, the five minute time-series data sets were further smoothed with a seven-point moving average, while maintaining a five minute sample interval. Time-series computations and rating curve development were performed using the Aquarius Whiteboard Time-Series Software (Aquatic Informatics, Inc., Vancouver, BC, Canada). Data summaries were exported for principal component analysis (PCA) and cluster analysis (CA) in IBM SPSS Statistics 20.0 (IBM Corporation, Armonk, NY, USA).

Parts of the statistical analysis and data summaries require daily values. To minimize the influence of the diurnal peak from the previous day, the time-series were divided based on the timing of diurnal minimum flow, which tended to occur between 06:00 and 08:00 Pacific Standard Time. For this study, 06:00 was used to divide the five minute time-series data into 'hydrologic days' (i.e. 06:00–05:59) whenever daily data were required.

Data analysis

The statistical analysis of the meteorological, pro-glacial hydrometric, and suspended sediment data was guided by the analysis of a similar data set by Orwin and Smart (2004) – for the nearby Small River Glacier (SRG), thereby enabling comparison – which is based on a pro-glacial hydrograph classification technique developed by Hannah *et al*. (2000). The analysis uses PCA and CA to reduce large time-series data sets into categories of similar data while maintaining as much of the underlying structure of the data as possible. Hannah *et al*. (2000) used the analysis to categorize discharge time-series data into categories of 'shape' and 'magnitude' based on the diurnal hydrograph. Orwin and Smart (2004) indicate that the analysis is applicable to any time-series data with an underlying cyclic structure, and expanded the analysis to include pro-glacial suspended sediment data. Through the analysis, they were able to infer controls on the pattern of suspended sediment transport using four separate classification procedures (Figure 3). The PCA and CA analyses were run on data matrices where 'cases' refer to rows of data categories down the *y*-axis; and 'variables' refer to columns of data categories across the *x*-axis. The following sub-sections describe the statistical procedures that were performed on the 2011 CCG pro-glacial data (i.e. as shown in Figure 3).

Meteorological periods

The 15-minute meteorological data sets were averaged over the hydrologic day (06:00–05:59) and a CA was run to group the daily data into categories of similar conditions. The CA of meteorological data included cases of daily values for the variables: mean, maximum, and minimum air temperature; total precipitation; mean relative humidity; total solar radiation; and mean wind speed. Air temperature records from the upper and lower AWS were averaged for the analysis. The data were standardized (*z*-scored) prior to running the CA using Ward's Method, and an agglomeration dendrogram was plotted to determine the number of meaningful clusters within the data. The raw data within each cluster were reviewed, and descriptive

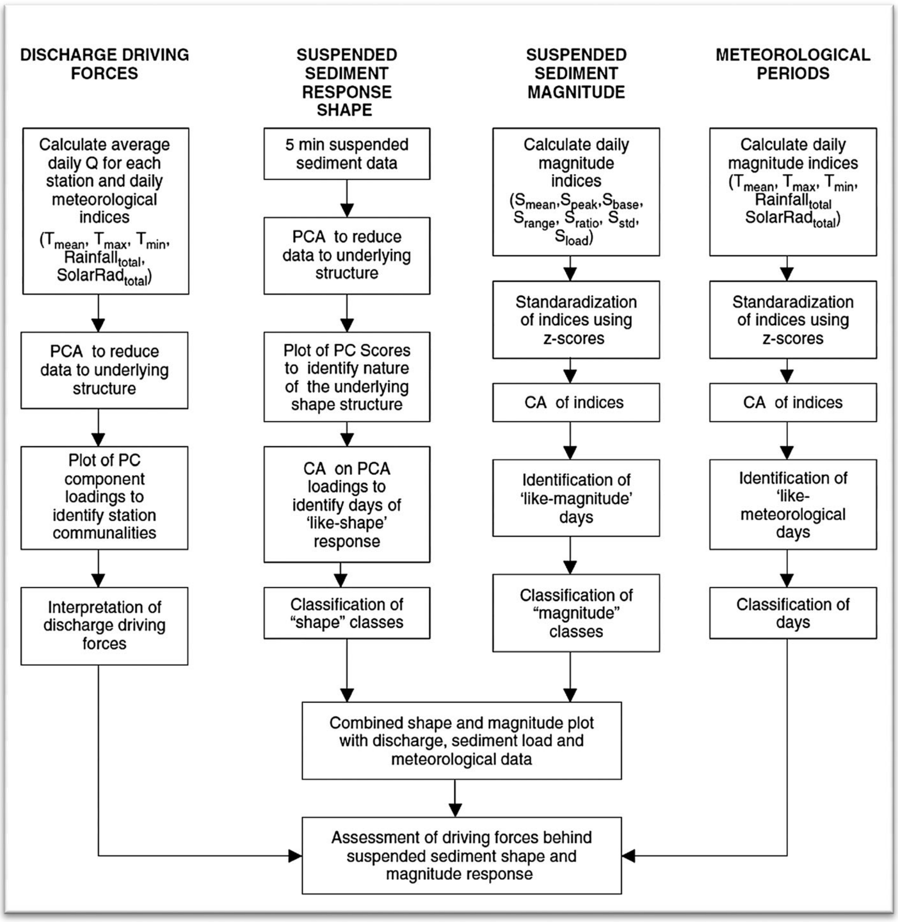

Figure 3. Flow chart detailing the classification procedure used to extract suspended sediment transfer patterns (source: Orwin and Smart 2004).

titles were assigned, which were broadly similar to those assigned by Orwin and Smart (2004).

Streamflow driving factors

To determine the main driving forces of Q (i.e. from glacial meltwater or precipitation), the input matrix for PCA had daily average Q for each site, total precipitation, solar radiation, average wind speed, and air temperature minimum, maximum and mean as variables, and hydrologic days as cases. The PCA was run using a VARIMAX orthogonal rotation with standard retention criteria. Low communality variables were removed from the analysis and the PCA was re-run on the remaining variables. The Kaiser–Mayer–Olkin (KMO) measure of sampling adequacy (Tabachnick and Fidell, 1989) was used to assess the correlation matrix and suitability of the data set for PCA. Parallel analysis was used to identify the statistically significant eigenvalue for the data (O'Connor, 2000). Components with significant eigenvalues were retained to assess the driving factors of Q and the proportion of variance in the data explained by each component. A bi-plot of the two dominant components was generated and descriptive titles (i.e. 'ablation' or 'rainfall') were assigned after assessing the data explained by the component.

Suspended sediment response shape

To assess the underlying suspended sediment response shape, an independent PCA was run on a data matrix with hydrologic days as variables and a five-minute time step as cases for SSC data at each site. The PCA was run using a VARIMAX orthogonal rotation with standard retention criteria. Parallel analysis was used to identify the statistically significant eigenvalue for the data (O'Connor, 2000). For each site, a scree plot was generated to confirm the break point in the principal components, and that components with eigenvalues > 1 were retained. Principal component loading scores were plotted against time to reveal the underlying shape of the five-minute SSC data for each site.

Days with similar diurnal suspended sediment response shape were identified by running a hierarchical CA on the principal component loading scores using Ward's Method. Observations were standardized (z-scored) to remove major variations in SSC magnitude. Low communality variables were removed and an agglomeration dendrogram was plotted to visually identify the number of clusters. The shape structure of the raw data in the clusters was examined and appropriate titles (i.e. 'diurnal' or 'irregular') were assigned.

Suspended sediment response magnitude

The classification of suspended sediment response magnitude was determined by running CA on a data matrix with daily SSC mean, minimum, maximum, range, standard deviation and daily total SSL as variables, with hydrologic days as cases for each site. Data were standardized (z-scored) prior to running the CA using Ward's Method, and an agglomeration dendrogram was plotted to visually identify the number of clusters. The magnitude structure of the raw data in the clusters was examined and appropriate titles (i.e. 'low', 'medium' or 'high') were assigned.

Results and Discussion

Meteorological conditions

The weather conditions over the first 24 days of the field season, from JD 195 to JD 218, were variable (Figure 4). Average daily temperatures tended to be < 8 °C and low to moderate precipitation was common. This period included one storm event on JD 211 when daily precipitation exceeded 30 mm. After JD 218, the weather conditions tended to persist for periods; there were three warmer and drier periods, and two cooler and wetter periods. There was another intense storm on JD 234 (Figure 4). During the onset of the intense rain event on JD 234, the tipping bucket rain gauge was damaged, and data for this event and thereafter were missed. Data for this event and the remainder of the field season were estimated from three nearby meteorological stations; two operated by Environment Canada (Cariboo Lodge near Valemount, EC ID 1171393; and Crescent Spur, EC ID 1092120) and one by the BC Ministry of Environment (McBride upper snow pillow, BC MOE ID 1A02P). A weighted average based on horizontal and vertical proximity to the study site was used. Fortunately, the remainder of the field season was dominated by a high pressure system and there was minimal precipitation. Field personnel were on site during both storm events and qualitative observations were made. The storm event on JD 211 was characterized by persistent precipitation throughout the day, while the storm event on JD 234 consisted of a series of intense squalls that began mid-afternoon and ended by early morning on JD 235. The onset of the event on JD 234 was synchronous with the diurnal peak, and Q was already moderate in response to warm weather on the previous two days.

The CA of meteorological data allowed the field season to be divided into four categories that, upon reviewing the raw data within the category, were described based on air temperature and precipitation conditions (Figure 4). Those categories and the percentage of the field season that they represent are: 'cold and wet' (17/60, 28%), 'warm and damp' (15/60, 25%), 'hot and dry' (26/60, 43%), and 'storm event' (2/60, 3%). These categories were used for comparison of Q and suspended sediment response under different meteorological conditions.

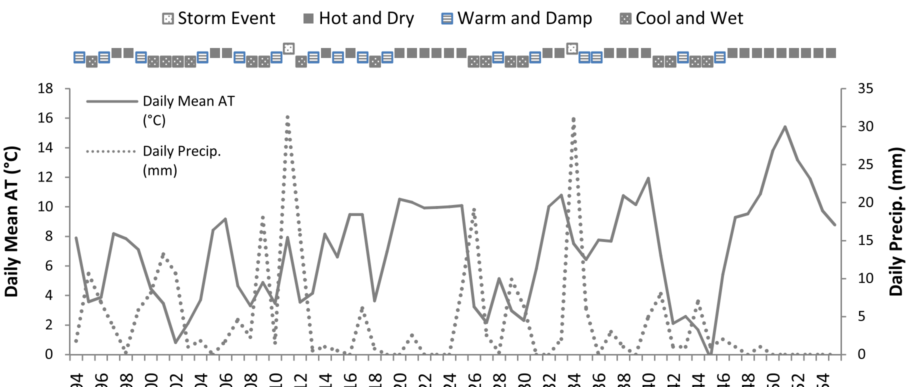

Figure 4. Mean daily air temperature and precipitation with results of cluster analysis for dominant meteorological conditions during the study period. Note: x-axis is in Julian Days. This figure is available in colour online at wileyonlinelibrary.com/journal/espl

Nine of the 'hot and dry' days occurred in early September when the approaching autumnal equinox limited the amount of daily insolation and the potential for ablation. Additionally, by this point in the field season, the annual snowpack had all but retreated from the pro-glacial zone and ablation zone of the glacier, leaving primarily ice melt to augment *Q*. Had this 'hot and dry' weather occurred earlier in the field season when the days were longer and annual snowpack was still present, the *Q* and SSC response could have been much different. Without these nine days in the data set, the field season was nearly balanced between the three main categories of meteorological conditions.

Streamflow

Streamflow (*Q*) during the field season was predominantly characterized by a diurnal pattern in response to air temperatures and meteorological conditions that cause snow and ice melt (Figure 5).

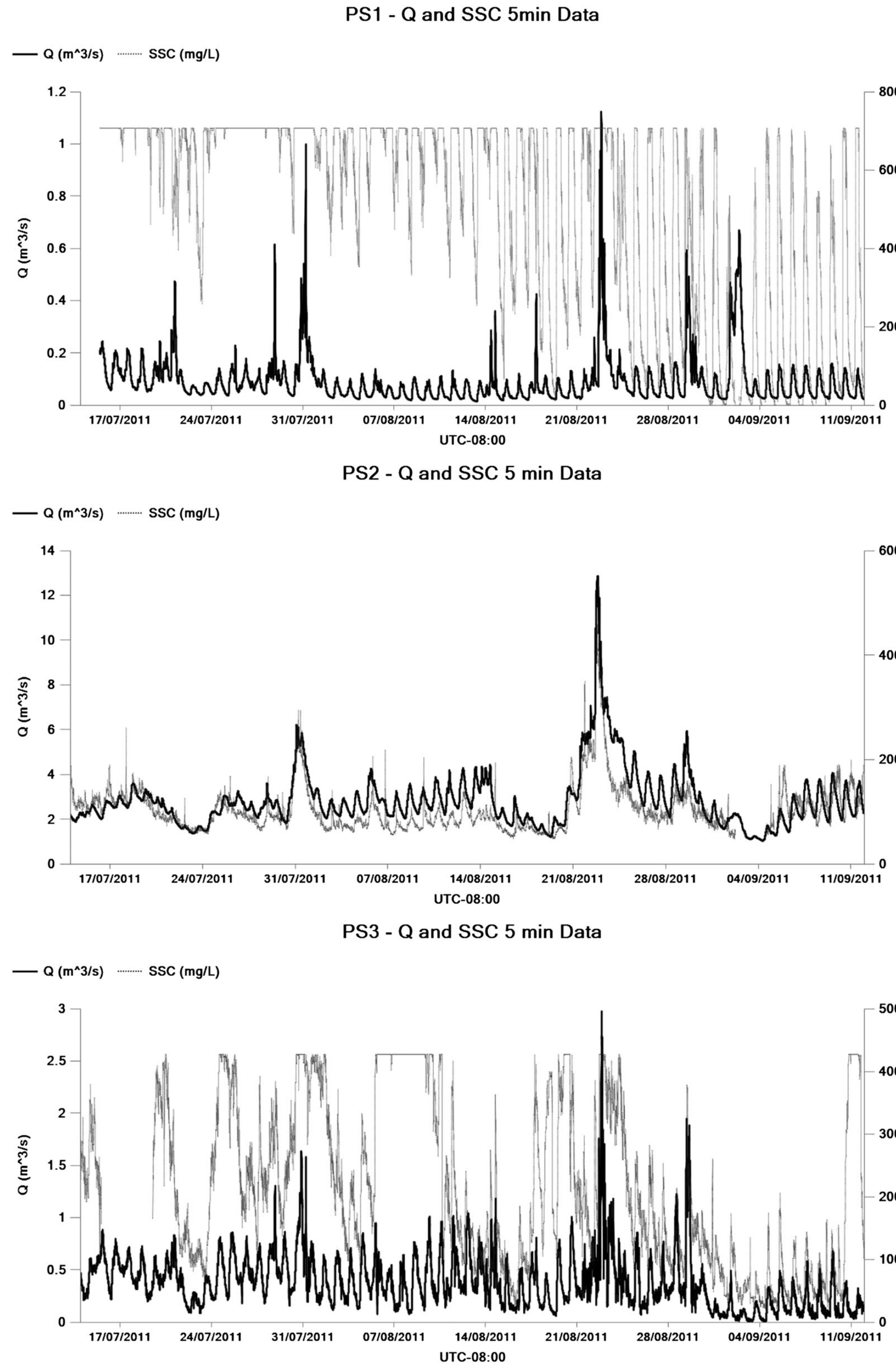

Figure 5. Streamflow (*Q*) and suspended sediment concentration (SSC) time-series (five minute data interval) from five pro-glacial monitoring sites, for the period Julian Day (JD) 195–JD 254, 2011. Scale of *y*-axis varies according to range of data.

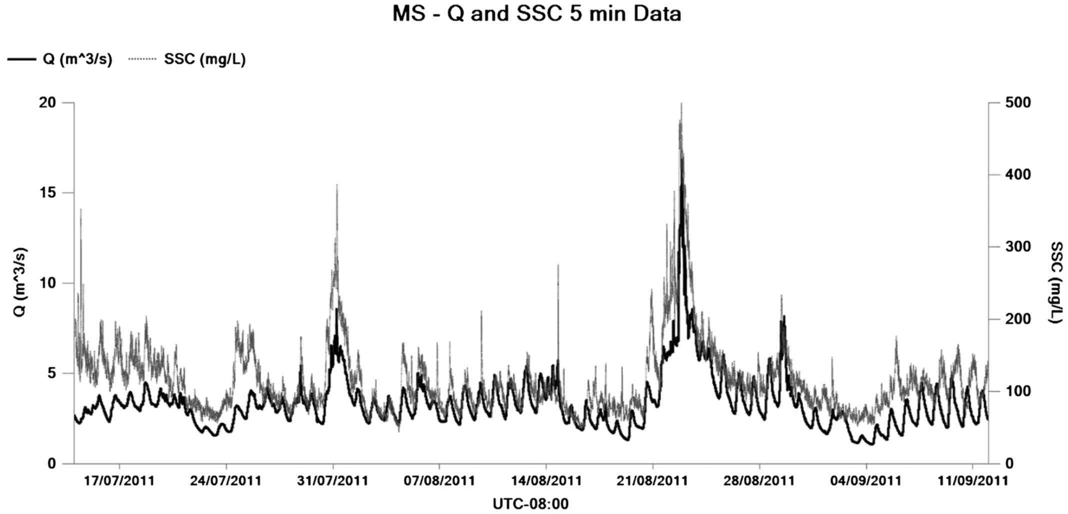

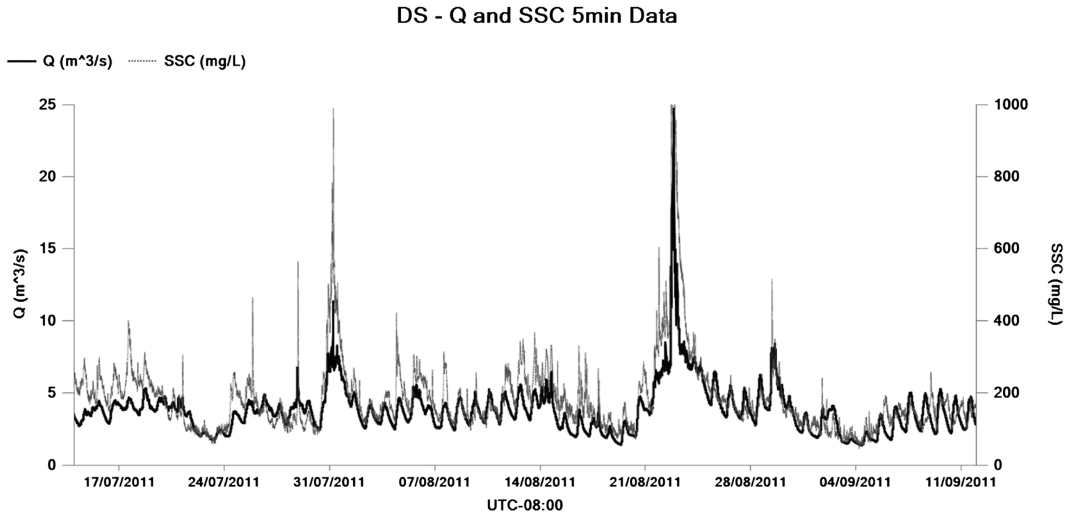

Figure 5. (Continued)

Increased Q due to precipitation events can be thought of as being superimposed on this underlying diurnal response pattern.

The PCA of Q and meteorological conditions reduced the data to their underlying components. The two dominant eigenvalues > 1 were used to generate a bi-plot, and descriptive titles were assigned (Figure 6). The KMO measure of sampling adequacy index for the correlation matrix was 0.532 which indicated that the PCA was a suitable analysis; as a rule of thumb, if the KMO is > 0.5, PCA is a suitable analysis (Tabachnick and Fidell, 1989).

The two components that were retained from the analysis explained 72% of the total variance in Q data (Figure 6). The first component was interpreted as 'rainfall' or stormy conditions and explained 42% of the variance in Q. The second component was interpreted as 'ablation' and explained 30% of the variance in Q. Distance from the origin (0.0, 0.0) was interpreted as dominance of the driving factor on Q pattern for the site. Orwin and Smart (2004) found that the two component solution explained 77% of the total variability in the data from the 2000 field season at SRG; 55% was attributed to 'ablation', and 22% was attributed to 'rainfall'. In the CCG analysis the days that were represented by 'rainfall' were not necessarily days with substantial precipitation, they may have just not scored as 'ablation' driven days because they were overcast, cool and/or windy; thus, stormy conditions may be an equally applicable title for the component. The greater influence of the 'rainfall' component on Q in the CCG analysis may be a result of the later field season (JD 194–JD 254 at CCG versus JD 188–JD 238 at SRG), and thus a lower influence of annual snowmelt ablation in the 2011 Q data for CCG than in the 2000 Q data for SRG (Orwin and Smart, 2004).

In general, all of the sites plot strongly positive on the 'rainfall' axis, but show less variation from the origin on the 'ablation' axis. Sites PS2, MS and DS were along the main stem

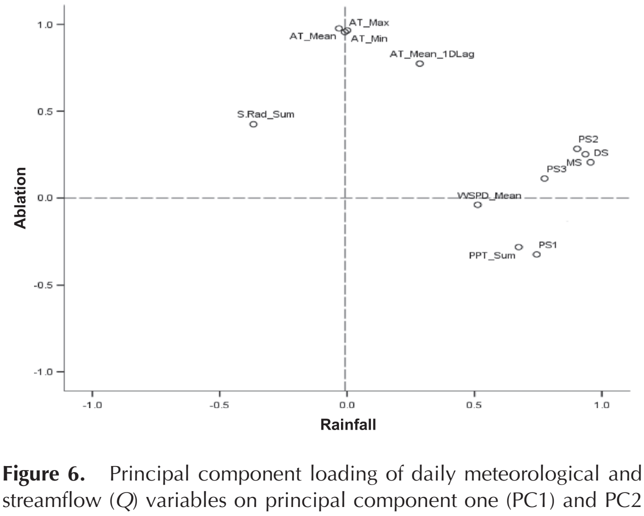

Figure 6. Principal component loading of daily meteorological and streamflow (Q) variables on principal component one (PC1) and PC2 explained 42% (PC1) and 30% (PC2) of the total variance in the principal component analysis (PCA). Distance of the variable from the origin indicates relative dominance of the Q generating processes; PC1 and PC2 were interpreted as 'Rainfall' and 'Ablation', and have been titled accordingly on the axes of the figure.

of the Castle Creek meltwater channel, and all plot close together, and were strongly influenced by 'rainfall' and moderately influenced by 'ablation'. As the distance from the glacier increased, the influence of 'ablation' on Q patterns decreased and the influence of 'rainfall' increased; which was consistent with the results of Orwin and Smart (2004). Although the PS3 catchment had the greatest percentage glacial cover, it was less influenced by 'ablation' and 'rainfall' than the sites along the main channel, which suggests a more stable source of flow from deeper within the glacier than the active ablation zone (Swift *et al.*, 2002). PS1 plots negatively on the 'ablation' axis, which was interpreted as a stronger influence of 'rainfall' on Q than 'ablation' due to the small proportion of glacierized catchment area.

The precipitation variable plotted positively on the 'rainfall' axis and negatively on the 'ablation' axis, while solar radiation plotted positively on the 'ablation' axis and negatively on the 'rainfall' axis; which was interpreted as ablation being generated by sunny days, and that cloudy days generated precipitation. The air temperature variables indicate a strong positive relation on the 'ablation' axis and near neutral on the 'rainfall' axis; which was interpreted as warm weather generated ablation, and that rainy weather was not necessarily cool. The wind speed variable plots neutral on the 'ablation' axis, which could be a result of net balance in the data, rather than no effect, and positive on the 'rainfall' axis, indicating that wind speed increased during rainy or stormy weather. The trend of katabatic winds would have been observed more strongly at the lower meteorological station; this trend was muted by averaging the wind speed data from the upper and lower meteorological stations. It is likely that wind speed from the lower meteorological station alone would have plotted more positively on the 'ablation' axis.

Suspended sediment concentration response pattern

Suspended sediment concentration (SSC) responded similarly to Q; however, there are several instances of striking independence between the SSC and Q time-series at each site (Figure 5). The 'shape' and 'magnitude' of suspended sediment response was categorized using PCA and CA. For this part of the analysis, the exceedances were left in the data sets; however, missing and partial days of data were omitted. The total number of useable days within the study period is reported in Table III.

Suspended sediment response shape

The PCA that was run on the five minute SSC data retained three components for each site. Principal loading scores on the three components were generated and plotted against time to reveal the underlying 'shape' of the components (Figure 7). Time is reported in decimal days counting up from zero, and data are for the hydrologic day (06:00–05:59). For instance, the first sample of the day is at 06:00, which is 6/24, or 0.25 of a day.

The percentage of data that was represented by each principal component is reported for each site in Figure 7. Since the analyses were run independently for each site, the 'shape' of the principal component was not necessarily comparable across sites; the days that make up the first principal component (PC1) at one site might fall into the second principal component (PC2) at another site. Overall, PC1 and PC2 represented an average of 36% and 21% of the data, the third principal component (PC3) represented an average of 8.5% of the data, and an average of 35% of the data was not represented by the any of the three principal components. All three principal components appeared to have a relatively well-defined pattern for PS1, PS3, MS and DS. The PC3 pattern appeared to be more stochastic for PS2, and appears to be double peaked at PS3, MS and DS. The results presented by Orwin and Smart (2004) were similar; PC1, PC2 and PC3 represented an average of 37%, 20%, and 10%, respectively, of their suspended sediment data and PC3 also showed a more irregular response pattern.

A CA was run on the principal component loading scores, and the two cluster solution was used to categorize days as 'diurnal' or 'irregular' suspended sediment response shape (Table IV). Comparisons of these results with the results from the regression score loading plots (Figure 7) confirm that PC1 and PC2 roughly represent the 'diurnal' data as a percentage, while PC3 and the remaining data that were not represented by a principal component make up the 'irregular' data. The distribution of 'diurnal' and 'irregular' response days is presented in Figure 8 with the hydrographs and sedigraphs, and Table IV shows the distribution within the meteorological categories.

Suspended sediment response magnitude

The CA of the SSC magnitude parameters separated the daily data into 'high', 'medium' and 'low' categories (Figure 8,

Table III. Turbidity (Tu) data summary for the pro-glacial monitoring sites for 2011 field season

	Site				
Data record	PS1	PS2	PS3	MS	DS
Total days with data record	60	63	62	62	64
Number of days JD 195–JD 254	58	60	60	60	60
Partial days	10	3[b]	2[b]	—	—
Partial day exceedance [d]	48	—	13	—	1
Missing days	2[a]	1[b]	3[b]	—	—
Full day exceedances [d]	4	—	2[c]	—	—
Useable days within JD 195–JD 254 [d]	58[a]	56[b]	53[b]	60	60
Percentage of record useable	97	89	85	97	94
Number of five minute data points	16134	16534	15567[c]	17280	17280
Number of five minute exceedances	6332	0	1707	0	33
Percentage of data within Tu range	61	100	89	100	100
Maximum SSC [d]	707.1		427.4		1009.1

[a]Late start of data collection.
[b]Low water.
[c]Two days of erroneous data excluded.
[d]Maximum suspended sediment concentration (SSC; mg l^{-1}) value as computed by regression equation.

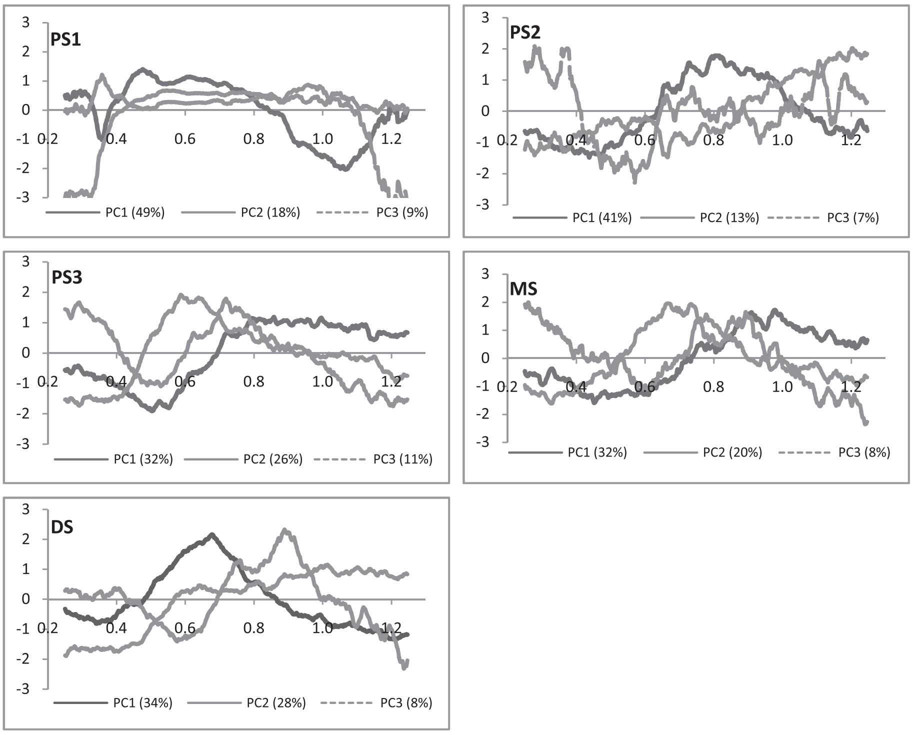

Figure 7. Principal component loading score plots for five minute suspended sediment concentration (SSC) data from each gauging station; all full hydrologic days of data were retained as variables for the analysis. Percentage of the data represented by each principal component is reported for each site. Time, on the *x*-axis, is reported in arbitrary decimal days (06:00 is 0.25 of the way through a regular day).

Table IV. Summary of suspended sediment 'shape' and 'magnitude' analysis for pro-glacial monitoring locations for monitoring period, Julian Day (JD) 195–JD 254

Site	Cluster classification	Cold and Wet (17 days)	Warm and Damp (15 days)	Hot and Dry (26 days)	Storm (two days)	Days (N) 60	Total days (N_T) 60
PS1	Diurnal (Irregular)	15 (1)	12 (2)	18 (8)	(2)	45 (13)	58
	High	10 (1)	8 (2)	5 (8)	(2)	23 (13)	58
	Medium	4	4	13	—	21	
	Low	1	—	—	—	1	
PS2	Diurnal (Irregular)	1 (15)	7 (7)	21 (3)	2	31 (25)	56
	High	(1)	(1)	1	2	3 (2)	56
	Medium	1 (6)	4 (1)	12 (2)	—	17 (9)	
	Low	(8)	3 (5)	8 (1)	—	11 (14)	
PS3	Diurnal (Irregular)	13 (4)	9 (4)	13 (8)	2	37 (16)	53
	High	7 (1)	4 (1)	2 (4)	2	15 (6)	53
	Medium	1	5 (1)	5 (3)	—	11 (4)	
	Low	5 (3)	(2)	6 (1)	—	11 (6)	
MS	Diurnal (Irregular)	2 (15)	10 (5)	23 (3)	2	37 (23)	60
	High	—	—	—	1	1	60
	Medium	(3)	(1)	3	1	4 (4)	
	Low	2 (12)	10 (4)	20 (3)	—	32 (19)	
DS	Diurnal (Irregular)	3 (14)	8 (7)	23 (3)	2	36 (24)	60
	High	(1)	—	—	2	2 (1)	60
	Medium	1 (3)	3 (2)	6 (2)	—	10 (7)	
	Low	2 (10)	25 (5)	17 (1)	—	24 (16)	

Table IV), and was a useful tool for looking at how the magnitude of SSC changed over the field season at a particular site. Sites MS and DS were dominated by 'low' magnitude response days, PS2 was dominated by 'medium' and 'low' response days, PS3 was split across the three magnitude categories, and PS1 had 'high' and 'medium' magnitude response days. Orwin and Smart (2004) report that on average 80% of their data fell into the 'low' magnitude category and 20% fell into the 'high' magnitude category.

Since each CA was independent from the other sites, the scale of the magnitude varies, which limits the ability to compare the results of this analysis across sites. For example, the mean SSC for a 'medium' day at PS2 was 112 mg l^{-1}, while the mean SSC of a 'medium' day at PS1 was 292 mg l^{-1}. A greater number of 'medium' and 'high' magnitude response days at PS2 (Tables IV and V) does not mean that there was more sediment transported at this site than at MS; it is more likely a result of lower peak sediment loads at PS2 that allow the scale of the analysis to be focused on a smaller range than at MS. The mean daily SSC for a 'high' magnitude day at PS2, MS and DS were 195, 336 and 449 mg l^{-1}, respectively (Table V). Similarly, a small amount of very high data could stretch the scale of the analysis so that the majority of the data would fall into a 'low' magnitude category;

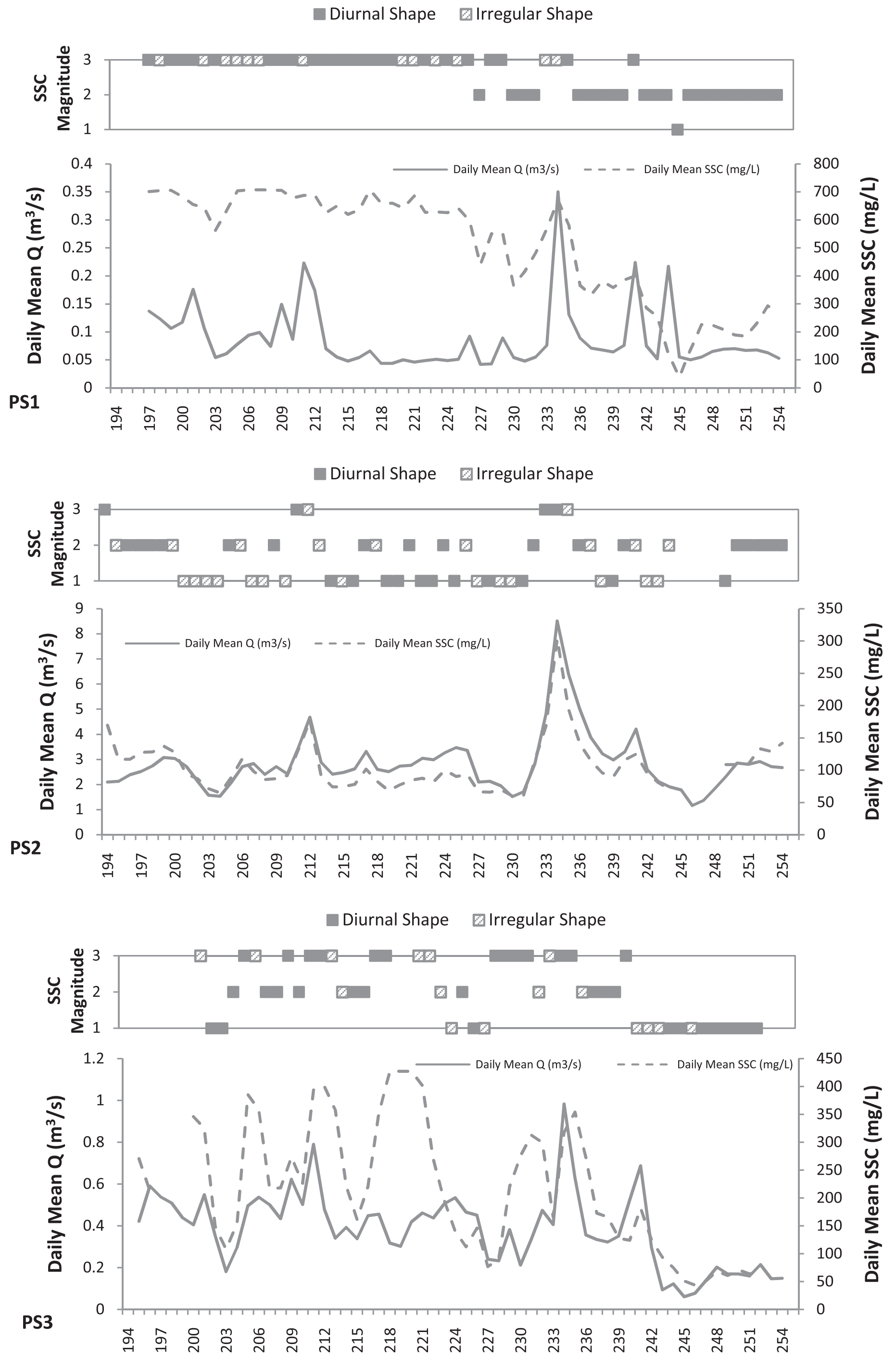

Figure 8. Composite figures showing suspended sediment shape (diurnal or irregular) and magnitude (1 = low; 2 = medium; 3 = high) classification results from principal component analysis and cluster analysis and daily mean streamflow (*Q*) and suspended sediment concentration (SSC) for each of the pro-glacial monitoring sites. PS1, PS2, and PS3 are missing days in the shape and magnitude classification due to low water, partial days of data, erroneous data or no data (see Table III). Note: *x*-axes in Julian Days.

in which case, the detail of the time-series data could become lost or obscured. Differences in scale between the sites were also reported for a similar analysis on the data from SRG by Orwin and Smart (2004), which they attributed to sediment availability in the contributing catchment area.

Suspended sediment load response to meteorological conditions

Suspended sediment load was computed from the five minute time-series data, and summarized into hydrologic days. The time-series were then divided into the categories determined through PCA and CA. The quantity of sediment generated under the various conditions was computed and summarized as daily averages (Table VI). The values are reported in kilograms per day for the specified category; totals can be computed by multiplying values in Table VI by the corresponding values for number of days in Table IV.

From the information in Table VI, it is possible to determine where, when and how much sediment was generated, transported, stored and evacuated from the basin during the 2011 field season. To simplify the information, it could be presented as percentage of total; however, the distribution of days across categories varied by site and is specific to the 2011 field season, which would make comparisons between locations or

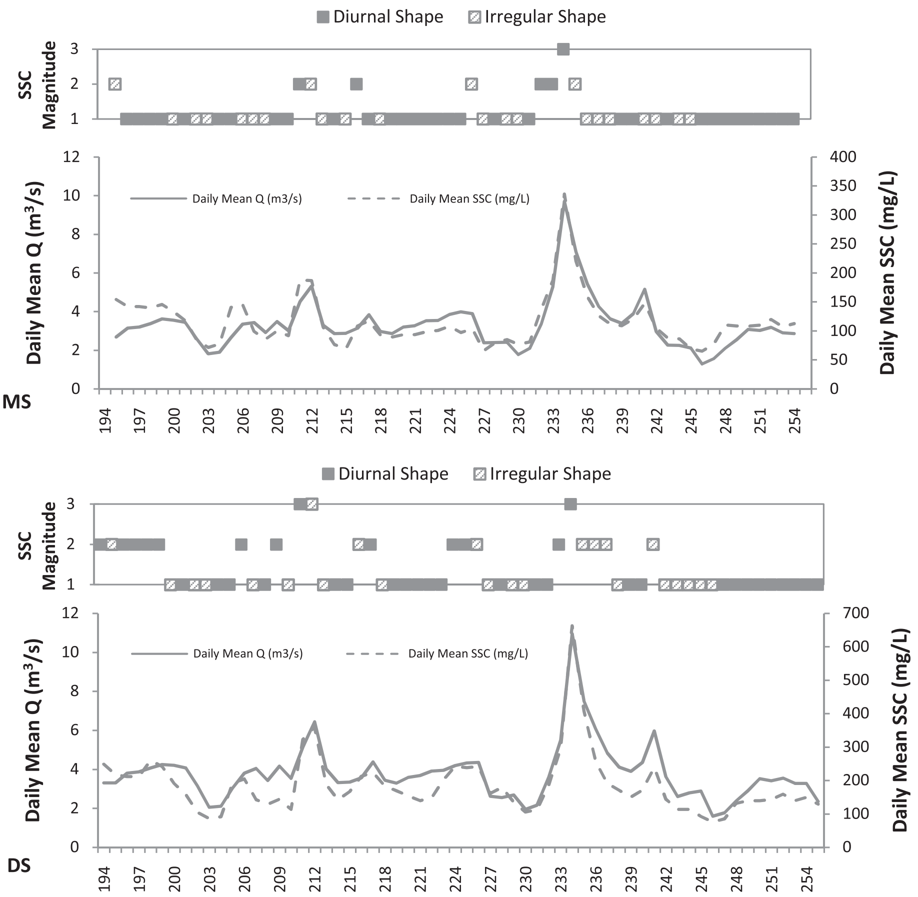

Figure 8. (Continued)

Table V. Summary of suspended sediment response magnitude parameters and cluster analysis results

Site	SSC Magnitude class	Average SSC_{min} (mg l^{-1})	Average SSC_{max} (mg l^{-1})	SSC_{mean} (mg l^{-1})	Average SSC_{range} (mg l^{-1})	Average $SSC_{Std.Dev.}$ (mg l^{-1})	Average standard SSC_{range} (ratio)	Average SSL (kg day^{-1})	Days (N)	Total days (N_T)
PS1	High	433 (168)	707 (0)	644 (63)	284 (168)	80 (55)	1.0 (1.0)	5619 (3698)	36	58
	Medium	16 (40)	683 (52)	292 (99)	667 (54)	233 (36)	27 (196)	2313 (577)	21	
	Low	0	122	38	146	41	6.0	640	1	
PS2	High	119(44)	356 (84)	196 (58)	236 (50)	58 (14)	2.2 (0.8)	108893 (68359)	5	56
	Medium	80 (17)	176 (32)	112 (19)	96 (35)	20 (8)	1.3 (0.6)	29072 (9564)	26	
	Low	65 (10)	111 (18)	81 (13)	45 (14)	9 (3)	0.7 (0.3)	17323 (5572)	25	
PS3	High	174 (92)	393 (70)	306 (90)	219 (81)	63 (33)	2.0 (1.6)	13387 (6898)	21	53
	Medium	102 (32)	319 (74)	199 (49)	216 (60)	54 (20)	2.3 (0.8)	7211 (2628)	15	
	Low	43 (28)	192 (78)	92 (40)	149 (71)	33 (16)	4.9 (3.3)	2817 (2305)	17	
MS	High	193	499	336	305	84	1.6	301577	1	60
	Medium	88 (30)	311 (72)	161 (39)	233 (53)	47 (12)	2.7 (0.7)	68120 (35730)	8	
	Low	74 (17)	147 (35)	103 (24)	73 (26)	16 (6)	1.0 (0.4)	28630 (13223)	51	
DS	High	211 (108)	968 (45)	449 (152)	757 (71)	189 (50)	5.0 (3.0)	367279 (249474)	3	60
	Medium	162 (41)	396 (116)	238 (53)	233 (120)	51 (25)	1.6 (1.2)	100484 (49369)	17	
	Low	97 (22)	210 (55)	143 (32)	113 (45)	26 (12)	1.2 (0.5)	41631 (15893)	40	

Note: Values computed from daily data. Standard deviations are reported in parentheses.

over different field seasons difficult; Hannah *et al.* (2000) also report this limitation with the analysis. As described previously, 'shape' and 'magnitude' parameters were essentially driven by hydro-meteorological conditions at the time of monitoring. Thus, the most applicable division of the field season is into the hydro-meteorological periods. From there, similar computations of totals and averages can be made, but reported in a simplified format that will be more useful for modelling applications, assessing subsequent years of data, or comparing data from other sites.

Suspended sediment load and Q in Table VII were computed as a percentage of the daily average at DS for the specified meteorological category; the daily average SSL and Q values for each meteorological category at DS were included for back calculation purposes. Differences in source contribution to the total SSL at DS during the defined hydro-meteorological categories can be compared in Table VII and Figure 9.

Mean daily SSL and Q were similar during 'cold and wet' and 'hot and dry' conditions at the catchment outlet, although the percentage contribution from the monitoring locations to the total at DS varies. Glacial melt decreased during 'cold and wet' conditions, and while precipitation activated some in-channel and pro-glacial sediment sources, low stream

Table VI. Summary of average suspended sediment load (in kg day^{-1}) for each sub-category

Site	Cluster classification	Cold and Wet	Warm and Damp	Hot and Dry	Storm	Weighted average	Average
PS1	Diurnal (Irregular)	4927 (5829)	3567 (4736)	2866 (4188)	(17200)	3740 (6400)	4336
	High	6430 (5829)	4320 (4736)	4044 (4188)	(17200)	5177 (6400)	5619
	Medium	2240	2061	2413	—	2313	2313
	Low	640	—	—	—	640	640
PS2	Diurnal (Irregular)	20774 (23451)	26874 (30702)	27595 (30822)	142879	34650 (26366)	30952
	High	(74606)	(109527)	74572	142879	120110 (92067)	108893
	Medium	20774 (26345)	37951 (23263)	28013 (32911)	—	29926 (27462)	29072
	Low	(14886)	12105 (16425)	21096 (26643)	—	18644 (16275)	17323
PS3	Diurnal (Irregular)	7625 (8329)	8568 (5267)	4642 (10877)	29600	7994 (8838)	8249
	High	10932 (15130)	11378 (10915)	11824 (12552)	29600	13659 (12709)	13387
	Medium	8460	6320 (9060)	5818 (9982)	—	6286 (9752)	7211
	Low	2829 (6062)	(547)	1268 (6863)	—	1978 (4357)	2817
MS	Diurnal (Irregular)	33109 (29683)	24089 (58396)	32791 (41514)	191799	39051 (37468)	38444
	High	—	—	—	301577	301577	301577
	Medium	(53905)	(138134)	54363	82021	61278 (74962)	68120
	Low	33109 (23627)	24089 (38462)	29555 (41514)	—	28069 (29574)	28630
DS	Diurnal (Irregular)	50233 (61070)	53448 (85171)	58527 (70122)	444324	78140 (69231)	74577
	High	(213187)	—	—	444324	444324 (213187)	367279
	Medium	56034 (95476)	82680 (203185)	93841 (74156)	—	86712 (120159)	100484
	Low	47332 (35537)	35908 (37966)	46063 (62054)	—	44053 (37953)	41613

Note: Averages for 'irregular' response shape data are reported in brackets. The values reported in the body of the table are arithmetic means for the given category. Weighted averages were used to account for the disproportionate number of days in each category for the 'shape' and 'magnitude', and total summary. Table IV reports the the number of days in each category.

Table VII. Percentage (%) of mean daily suspended sediment load (SSL) and streamflow (Q) relative to the distal site (DS) during meteorological periods determined by principal component analysis (PCA)

Meteorological period	Cold and Wet 28% (17 days)		Warm and Damp 25% (15 days)		Hot and Dry 44% (26 days)		Storm 3% (two days)		Seasonal 100% (60 days)	
Site	Percentage of mean SSL at DS	Percentage of mean Q at DS	Percentage of mean SSL at DS	Percentage of mean Q at DS	Percentage of mean SSL at DS	Percentage of mean Q at DS	Percentage of mean SSL at DS	Percentage of mean Q at DS	Percentage of mean SSL at DS	Percentage of mean Q at DS
PS1	8	3	5	2	6	2	4	4	6	2
PS2	39	71	42	76	47	77	32	75	42	75
PS3	13	10	11	10	12	10	7	11	11	10
∑ PS1 + PS2 + PS3	61	84	59	87	64	89	43	89	59	87
MS	51	84	52	88	56	89	43	88	52	87
DS[a]	100 (59158)	100 (3.60)	100 (68252)	100 (3.69)	100 (59865)	100 (3.69)	100 (444324)	100 (8.05)	100 (74577)	100 (3.81)

[a]Mean SSL (kg day^{-1}) and Q (m^3 s^{-1}) have been included for DS for back calculation purposes

competency allowed storage on the outwash fan complex. There was a greater contribution from PS2 during 'hot and dry' conditions in response to ablation. Mean Q at DS was similar for 'warm and damp' and 'hot and dry', but mean SSL was greater for 'warm and damp' conditions and less SSL was derived from the three proximal sites. Aside from inputs downstream of MS, PS2 contributes the majority of the sediment load throughout the study period, varying between 32% during 'storm' events and 47% during 'hot and dry' periods (Figure 9).

The SSL increased significantly in the reach between MS and DS (MS–DS) for all of the hydro-meteorological periods; a minimum of 44% during 'hot and dry' conditions and a maximum of 57% during 'storm' events (Figure 9). The main source of sediment in the MS–DS reach was likely to be the main tributary stream in the study area which is confluent with the main stem of Castle Creek ~150 m upstream of DS (Figure 1). This tributary drains a small cirque glacier on the adjacent peak and the western slope of the pro-glacial zone (Figure 1). Field observations found abundant unconsolidated sediment within and adjacent to the meltwater stream flowing from the cirque glacier. It was not possible to adequately monitor SSL from the tributary during the 2011 field season due to low flow volume and high bedload transport. However, the main channel in the MS–DS reach was well established, and it was presumed that the majority of the SSL increase in the reach was from the tributary stream; diffuse para-glacial and channel marginal sediment sources within the reach would only be activated by snowmelt, intense precipitation or very high Q. As a seasonal average, there was a ~13% increase in flow and a ~48% increase in SSL in the MS–DS reach (Table VII and Figure 9).

The sum of the SSL from the three proximal streams was greater than that of MS for 'cold and wet', 'warm and damp', and 'hot and dry' conditions, indicating that there was sediment storage upstream of MS. Based on site observations and the longitudinal profile (Figure 2), storage predominantly occurred on the low gradient outwash fan complex immediately upstream of MS. The amount of storage on the outwash fan varied slightly over the three main hydro-meteorological periods, and was ~7% as an average for the study period. However, during the observed 'storm' events, the SSL output from the three proximal stations was equal to the SSL at MS, indicating that sediment storage on the outwash fan complex was balanced

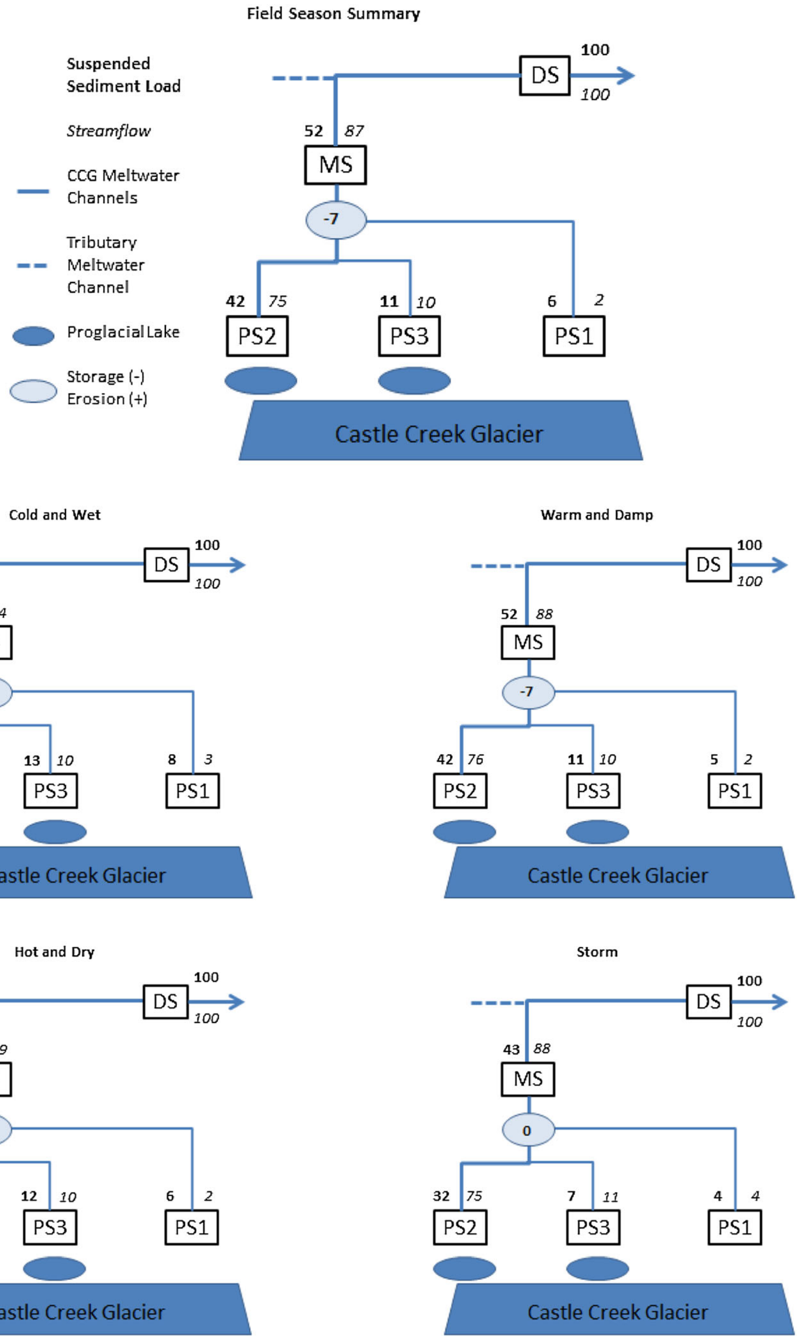

Figure 9. Schematic diagram of percentage (%) contribution of suspended sediment load (SSL) and streamflow (Q) relative to the total at the downstream gauging site (DS) over the 2011 field season and during the four defined hydro-meteorological categories. This figure is available in colour online at wileyonlinelibrary.com/journal/espl

with sediment evacuation and other sediment contributions upstream of MS triggered by high stream competency.

While the balance of SSL and Q contribution shifts moderately under meteorological and Q conditions that account for 97% of the study period, 'storm events' were remarkably different as sediment contribution from the proximal sites became less important when channel processes, slope inputs and erosion of valley sandur were more active. During the two storm days that accounted for 3% of the study period, SSL and Q at DS were 596% and 211%, respectively, of the seasonal average. However, the percentage of the total SSL that was derived downstream of MS increased to 57% as diffuse and point sources of sediment within the MS–DS contributing area were triggered by intense precipitation and high water levels. Interestingly, the proportion of Q input downstream of MS was similar to other hydro-meteorological periods. Five grab samples were collected in the MS–DS catchment as the JD 234 event peaked. Two were collected from ephemeral channels that drained directly into Castle Creek, one upstream of the tributary, and one downstream of the tributary; they were measured at ~3600 mg l^{-1} and ~2000 mg l^{-1}, respectively. The grab sample from the tributary was measured at ~4200 mg l^{-1}, and the main flow of Castle Creek upstream and downstream of the confluence with the tributary was measured at ~1300 mg l^{-1} and ~2700 mg l^{-1}, respectively. These peak values are comparable to those observed by other researchers (Gurnell *et al.*, 1996; Hodson *et al.*, 1998), but much less than the ~12 000 mg l^{-1} reported by Orwin and Smart (2004).

In Table VIII, values were computed based on the total SSL and mean Q for the study period to show the contribution during the specified meteorological category for each of the sites. Interestingly, ~20% of the total seasonal SSL at DS was evacuated during the 'storm' events, which was ~4% higher than PS2 and MS (Table VIII). The SSL increase in the MS–DS reach was attributed to the contribution of sediment from diffuse pro-glacial sources via ephemeral channels and the activation of sediment sources along the channel of the tributary stream. PS1 and PS3 had a lower percentage of their total SSL transported during 'storm' events than PS2, which is likely because of the dominance of bedrock in the PS1 catchment and glacial ice in the PS3 catchment, and because of lower abundance of sediment sources that are activated by 'storm' events in these catchments. The response pattern of MS was very similar to PS2 because 75% and 86%, respectively, of the total SSL and *Q* were derived from PS2. The SSL at PS2 showed a greater increase with 'storm' events than the other proximal sites because unconsolidated extra-channel sediment sources proximal or adjacent to the glacier were activated by precipitation and increased streamflow.

Daily SSY in Table IX was computed by dividing the mean sediment load for a given period (Table VII) by the contributing catchment area (Table I). For total yield, the mean daily SSY values are multiplied by the respective number of days of observation in the category (note that some sites are missing days, as reported in Table III). Interestingly, the SSY of the proximal sites tended to be greater than the SSY of MS. However, SSY between MS and DS increased with catchment area, which, as expected (Church and Slaymaker, 1989; Gurnell *et al*., 1996; Schiefer *et al*., 2001; Tunnicliffe and Church, 2011), disagrees with conventional sediment yield models (Syvitski and Milliman, 2007). During 'cold and wet' conditions the SSY at PS1 was greater than PS2, while it was less than PS2 for the other three meteorological conditions. SSY at MS was typically less than any of the proximal sites, indicating sediment storage within the pro-glacial channel network upstream of MS. The effect of 'storm' events on SSY was striking; compared to the mean for the study period, the minimum increase was 260% for PS3 and the maximum increase was 496% for DS. The downstream trend of increasing relative SSY during 'storm' events was likely because of ephemeral stream inputs from diffuse pro-glacial sediment sources during the events. Warburton (1990) found that a large proportion of the SSY can be generated in a short period of high stream competency, and Orwin and Smart (2004) also found that sediment was evacuated during storm events. This triggered response from the pro-glacial zone should be expected to continue, in declining magnitude, until the end of the para-glacial period (Church and Ryder, 1972; Church and Slaymaker, 1989; Gurnell *et al*., 1996; Ballantyne, 2002).

Pro-glacial suspended sediment budget

Based on the preceding analysis and field observations, a basic pro-glacial suspended sediment flux budget was developed to ascribe SSL to various sources based on the parameters defined by Warburton (1990). It was assumed that the error was normally distributed within the data and that the relative accuracy was valid. Again, it is important to emphasize that the sediment budget only applies to the study period, which represents part of the ablation season. The SSL contribution from the proximal sites was a combination of direct input from the glacier (GL), and input from moraine deposits at the terminus (MD). Based on field observations, the SSL for PS1 was predominantly from MD, while PS2 was mostly (80%) GL and PS3 may be split equally. Change in valley sandur (ΔVS) occurred on the outwash fan upstream of MS. With the exception of storm events, there was sediment stored upstream of MS, which can be defined as the difference between the input of sediment from the proximal sites and the amount of sediment measured at MS. The increase in the MS–DS reach was substantial throughout the field season. Based on field observations and accepting the limitations of the monitoring programme (cf. Gurnell *et al*., 1992), the increase in the MS–DS reach was attributed to tributary channel inputs (TR) with the exception of 'storm' events when ephemeral channels were observed to be actively contributing to SSL, and thus a portion of SSL would be from ΔVS. Direct hillslope inputs (SL) were observed along the right bank of the meltwater channel, upstream from the outwash fan and immediately downstream from the confluence of PS2 and PS3. The SL contribution is typically small, but episodic increases can be expected when triggered by high streamflow or spring snowmelt and freeze–thaw cycles. The total yield (*Y*) from the pro-glacial catchment was measured at DS. Following this premise, the suspended sediment budget for the CCG pro-glacial zone can be defined as:

$$\begin{aligned} Y\,(100\%) = {} & \mathrm{GL}\,(39\%) + \mathrm{MD}\,(20\%) + \Delta\mathrm{VS}\,(-7\%) \\ & + \mathrm{SL}\,(0.5\%) + \mathrm{TR}\,(49\%) \end{aligned} \tag{1}$$

Values were used directly or subdivided, as stated in the preceding paragraph, from the percentage of mean daily SSL and, following the same premise, a suspended sediment budget could be drawn for any of the hydro-meteorological categories (Table VII). In the overall suspended sediment budget for the CCG pro-glacial zone, GL and MD in the active meltwater channels at the snout of the glacier accounted for 59% of the SSL input. For the budget, ΔVS was computed as −7%, showing sediment storage on the outwash fan complex upstream of MS. The difference between MS and DS was 49% as an average, and attributed to TR; however, this reach was not adequately quantified and a portion can be expected to be generated from ΔVS during snowmelt, 'storm' events and high flow.

Table VIII. Meteorological summary of suspended sediment load (SSL) and streamflow (*Q*) for each site

Meteorological period	Cold and Wet 28% (17 days)		Warm and Damp 25% (15 days)		Hot and Dry 44% (26 days)		Storm 3% (two days)		Seasonal 100% (60 days)	
Site	Percentage of seasonal SSL	Percentage of seasonal Q	Percentage of seasonal SSL	Percentage of seasonal Q	Percentage of seasonal SSL	Percentage of seasonal Q	Percentage of seasonal SSL	Percentage of seasonal Q	Total SSL (t)	Mean Q ($m^3 s^{-1}$)
PS1	32	37	21	19	34	34	14	11	251	0.09
PS2	22	25	23	25	39	43	17	7	1733	2.85
PS3	30	27	23	24	34	41	14	8	437	0.38
∑ PS1 + PS2 + PS3	24	26	23	24	37	43	16	7	2421	3.36
MS	22	26	23	24	38	43	17	7	2307	3.32
DS	23	27	23	24	35	42	20	7	4475	3.81

Note: Values computed as a percentage of the seasonal total SSL and seasonal mean *Q*.

Table IX. Suspended sediment yield (SSY) for the Castle Creek Glacier catchment during the 2011 field season, expressed as mean daily SSY (in t km^{-2} day^{-1}) and total SSY (in t km^{-2}) (in parentheses) for each sub-basin

Site (km^2)	Cold and Wet (17 days) Mean daily (Total)	Warm and Damp (15 days) Mean daily (Total)	Hot and Dry (26 days) Mean daily (Total)	Storm (two days) Mean daily (Total)	Seasonal (60 days) Mean daily (Total)
PS1 (1.24)	4.01 (64.3)	3.00 (42.0)	2.64 (68.6)	13.9 (27.7)	3.49 (202)
PS2 (9.36)	2.48 (39.7)	3.08 (43.1)	2.99 (71.8)	15.3 (30.6)	3.31 (185)
PS3 (1.73)	4.49 (76.3)	4.37 (56.8)	4.05 (85.0)	17.1 (34.2)	4.76 (253)
MS (12.69)	2.37 (40.3)	2.80 (42.0)	2.66 (69.3)	15.1 (30.3)	3.03 (182)
DS (15.68)	3.77 (64.1)	4.35 (65.3)	3.82 (99.2)	28.3 (56.6)	4.76 (285)

Intensive field measurements were conducted by Warburton (1990) to define the pro-glacial fluvial sediment budget for JD 134–JD 211 of the 1987 ablation season at the Bas Glacier d'Arolla, Switzerland. The sediment yield was measured at proximal and distal ends of a 300 m pro-glacial reach. At the distal site, the catchment area was ~8 km^2 and 70% glaciated. Using various sampling approaches, *Y*, SL, TR, MD and ΔVS were measured or estimated. Pro-glacial sediment sources contributed 23% of the sediment received at the catchment outlet, and 95% of that contribution was generated from bank and channel erosion of valley sandur during a short period of meltwater flooding from JD 197 to JD 199. While SL and TR accounted for a small percentage of the total SSY, the GL and MD contribution accounted for ~77%. The ΔVS was of overwhelming importance in modifying the sediment load from GL and four basic fluvial process subsets were identified: (1) channel marginal; (2) channel; (3) hillslope; (4) slopewash. Since the GL component was estimated by quantifying the other variables and subtracting their total from the overall sediment yield, *Y*, the budget was not truly 'closed', and the cumulative error in the measurement of the other terms of the equation made the estimate precise to only ± 26% (Warburton, 1990).

Orwin and Smart (2004) found that SL and ΔVS in the pro-glacial zone were the source of 80% of the suspended sediment flux for the central stream, and 30% for the north stream during the 2000 field season at SRG. They cite sediment availability within the pro-glacial channels, SSC and *Q* of glacial inputs, and contribution from extra-channel sediment sources as key differences between the streams they monitored.

The SRG is a small (~7 km^2) cirque glacier with a relatively steep and small pro-glacial zone (~14% and 2 km^2) compared to that of CCG (~3% and 6 km^2), which is an alpine valley glacier (~16 km^2). Also, the de-glacierized study area at SRG had a greater elevation range (~450 m) compared to CCG (~70 m). The differences in the characteristics of the glacier and study site may partially explain the contrasting results. However, inter-annual variability of hydro-meteorological conditions and antecedent conditions, such as seasonal snowpack, can strongly influence pro-glacial *Q* and SSC which would affect the results of the analyses and thus comparisons between different sites and years of data (Gurnell *et al.*, 1996; Swift *et al.*, 2002; Richards and Moore, 2003; Cockburn and Lamoureux, 2008; Haritashya *et al.*, 2010). For instance, a pilot study at the CCG in 2008, based on monitoring of *Q* and SSC at only three sites over 34 days, found a 35% increase in the MS–DS reach (Stott *et al.*, 2009); in 2011 the increase in that reach was 49%. The early study also documented that the reach between the glacier snout site and MS was a net sediment source; although the area immediately in front of the snout in 2008 was considerably different than that in 2011. This helps to illustrate the dynamic nature of the pro-glacial zone over a short period, and the need for further monitoring at this and other study areas.

Conclusions and Perspective

The data collected from the July–September part of the 2011 ablation season showed that sub-glacial processes and moraine deposits exposed within the last few years were the dominant control on sediment flux patterns in the pro-glacial zone of the CCG. The meteorological conditions that drive *Q* and suspended sediment response will temporally vary, and further investigation would aid in the assessment of inter-annual variability. However, the results of the 'shape' and 'magnitude' analysis of the suspended sediment response pattern under the defined hydro-meteorological categories can be summarized for the sites along the main Castle Creek meltwater channel as: 'warm and damp' conditions generated a mixed response pattern that was influenced by antecedent conditions; 'hot and dry' conditions generated a strong diurnal response pattern that evolved through the season as annual snow cover waned; and, 'cold and wet' conditions and 'storm events' tended to generate irregular data. SSY increased by ~500% of the seasonal mean during 'storm' events, which represented 3% of the data set. As such, the findings support our two hypotheses. The dominant source(s) of sediment to the pro-glacial channel will evolve as the glacier retreats (or advances) and new sediment sources become active while older sources become exhausted or stabilized. However, episodic pulses of high sediment loads triggered by storm events and high *Q* are likely to continue throughout the para-glacial period.

The similarity and contrast of these results with the findings of other researchers, in addition to an early pilot study at this site, highlight the importance of seasonal conditions and site specific characteristics in determining the suspended sediment flux patterns. Additional research in targeted pro-glacial areas following this spatially distributed monitoring approach and analysis technique (Hannah *et al.*, 2000; Orwin and Smart, 2004) would help establish glacial input end members for larger sediment budget and climate change models.

Acknowledgements—MSL and PNO would like to acknowledge funding via a Forest Renewal BC operating grant, an NSERC Discovery grant, and a UNBC Seed Grant. BF and TAS wishes to acknowledge funding from a Liverpool John Moores University (LJMU) Learning and Teaching Award which partly funded this expedition. Cariboo Alpine Mesonet equipment purchases were supported by the Canada Foundation for Innovation, the British Columbia Knowledge Development Fund, and UNBC; additional funding was provided by the Canadian Foundation for Climate and Atmospheric Sciences through the Western Canadian Cryospheric Network, NSERC, and the Canada Research Chair programme of the Government of Canada to SJD. Thanks are extended to John Rex, Scott Jackson and James Jacklin (BC Ministry of Forests, Lands and Natural Resource Operations) for the use of ISCO water samplers, Analite turbidity probes and data loggers, to Maud Barrel, Sonja Ostertag and Natalie Vogt for assistance with fieldwork, and to Matt Beedle and Leticia Gaspar for assistance with the preparation of some of the diagrams. The authors thank the staff at UNBC's Quesnel River Research Centre (QRRC) for supporting the laboratory work associated with this study and for essential field equipment loan. This work benefited from discussions with Jeff Warburton. This contribution represents part of the QRRC publication series.

References

Ballantyne CK. 2002. A general model of paraglacial landscape response. *The Holocene* **12**: 371–376.

Beedle MJ, Menounos B, Luckman BH, Wheate R. 2009. Annual push moraines as climate proxy. *Geophysical Research Letters* **36**: L20501. DOI: 10.1029/2009GL039533

Bolch T, Menounos B, Wheate R. 2010. Landsat-based inventory of glaciers in western Canada, 1985–2005. *Remote Sensing of the Environment* **114**: 127–137.

Church M, Ryder JM. 1972. Paraglacial sedimentation: a consideration of fluvial processes conditioned by glaciation. *Geological Society of America Bulletin* **83**(10): 3059–3072.

Church M, Slaymaker O. 1989. Disequilibrium of Holocene sediment yield in glaciated British Columbia. *Nature* **337**(6206): 452–454.

Cockburn JMH, Lamoureux SF. 2008. Hydroclimatic controls over seasonal sediment yield in two adjacent high arctic watersheds. *Hydrological Processes* **22**: 2013–2027.

Collins M, Knutti R, Arblaster J, Dufresne J-L, Fichefet T, Friedlingstein P, Gao X, Gutowski WJ, Johns T, Krinner G, Shongwe M, Tebaldi C, Weaver AJ, Wehner M. 2013. Long-term climate change: projections, commitments and irreversibility. In *Climate Change 2013: The Physical Science Basis. Contribution of Working Group I to the Fifth Assessment Report of the Intergovernmental Panel on Climate Change*, Stocker TF, Qin D, Plattner G-K, Tignor M, Allen SK, Boschung J, Nauels A, Xia Y, Bex V, Midgley PM (eds). Cambridge University Press: Cambridge.

Déry SJ, Clifton A, MacLeod S, Beedle MJ. 2010. Blowing snow fluxes in the Cariboo Mountains of British Columbia, Canada. *Arctic, Antarctic and Alpine Research* **42**: 188–197.

Déry SJ, Hernández-Henríquez MA, Owens PN, Parkes MW, Petticrew EL. 2012. A century of hydrological variability and trends in the Fraser River Basin. *Environmental Research Letters* **7**(2): 024019. DOI: 10.1088/1748-9326/7/2/024019

Filliben JJ, Devaney J. 2013. Critical values of the normal PPCC distribution. NIST/SEMATECH e-Handbook of Statistical Methods. http://www.itl.nist.gov/div898/handbook/eda/section3/eda3676.htm [1 March 2014].

Fraser Basin Council (FBC). 2008. Fraser Basin Council: Vancouver, BC. http://www.fraserbasin.bc.ca [5 December 2011].

Gurnell AM, Clark MJ, Hill CT, Greenhalgh J. 1992. Reliability and representativeness of a suspended sediment concentration monitoring programme for a remote alpine proglacial river. In *Erosion and Sediment Transport Monitoring in River Basins*, Bogen J, Walling DE, Day T (eds), IAHS Publication 210. IAHS Press: Wallingford; 191–200.

Gurnell AM, Edwards PJ, Petts GE, Ward JV. 1999. A conceptual model for an alpine proglacial river channel evolution under changing climatic conditions. *Catena* **38**: 223–242.

Gurnell AM, Hannah D, Lawler D. 1996. Suspended sediment yield from glacier basins. In *Erosion and Sediment Yield: Global and Regional Perspectives*, Walling DE, Webb BW (eds), IAHS Publication 236. IAHS Press: Wallingford; 97–104.

Hammer KM, Smith ND. 1983. Sediment production and transport in a proglacial stream: Hilda Glacier, Alberta, Canada. *Boreas* **12**: 91–106.

Hannah DM, Smith BPG, Gurnell AM, McGregor GR. 2000. An approach to hydrograph classification. *Hydrological Processes* **14**: 317–338.

Haritashya UK, Kumar A, Singh P. 2010. Particle size characteristics of suspended sediment transported in meltwater from the Gangotri Glacier, central Himalaya – an indicator of subglacial sediment evacuation. *Geomorphology* **122**: 140–152.

Hodgkins R. 1999. Controls on suspended sediment transfer at a high-Arctic glacier determined from statistical modelling. *Earth Surface Processes and Landforms* **24**: 1–21.

Hodgkins R, Cooper R, Wadham J, Tranter M. 2003. Suspended sediment fluxes in a high-Arctic glacierised catchment: implications for fluvial sediment storage. *Sedimentary Geology* **162**: 105–117.

Hodson A, Gurnell A, Tranter M, Bogen J, Hagen JO, Clark M. 1998. Suspended sediment yield and transfer processes in a small high-Arctic glacier basin, Svalbard. *Hydrological Processes* **12**: 73–86.

Intergovernmental Panel on Climate Change (IPCC). 2013. *Climate Change 2013: The Physical Science Basis. Contribution of Working Group 1 to the Fifth Assessment Report of the Intergovernmental Panel on Climate Change*, Stocker TF, Qin D, Plattner GK, Tignor M, Allen SK, Boschung J, Nauels A, Xia Y, Bex V, Midgley PM (eds). Cambridge University Press: Cambridge; 1535 pp.

Jacobs JL, Dinman JD. 2013. Systematic analysis of bicistronic reporter assay data. Online tutorial. http://dinmanlab.umd.edu/statistics/tutorial.html#0 [2 April 2013].

Kirtman B, Power SB, Adedoyin JA, Boer GJ, Bojariu R, Camilloni I, Doblas-Reyes FJ, Fiore AM, Kimoto M, Meehl GA, Prather M, Sarr A, Schär C, Sutton R, van Oldenborgh GJ, Vecchi G, Wang HJ. 2013. Near-term climate change: projections and predictability. In *Climate Change 2013: The Physical Science Basis. Contribution of Working Group I to the Fifth Assessment Report of the Intergovernmental Panel on Climate Change*, Stocker TF, Qin D, Plattner G-K, Tignor M, Allen SK, Boschung J, Nauels A, Xia Y, Bex V, Midgley PM (eds). Cambridge University Press: Cambridge.

Milner AM, Brown LE, Hannah DM. 2009. Hydroecological response of river systems to shrinking glaciers. *Hydrological Processes* **23**: 62–77.

Moore RD, Fleming SW, Menounos B, Wheate R, Fountain A, Stahl K, Holm K, Jakob M. 2009. Glacier change in western North America: influences on hydrology, geomorphic hazards and water quality. *Hydrological Processes* **23**: 42–61.

Navratil O, Esteves M, Legout C, Gratiot N, Nemery J, Willmore S, Grangeon T. 2011. Global uncertainty analysis of suspended sediment monitoring using turbidimeter in a small mountainous river catchment. *Journal of Hydrology* **398**: 246–259.

O'Connor BP. 2000. SPSS and SAS programs for determining the number of components using parallel analysis and Velicer's MAP test. *Behavior Research Methods, Instrumentation, and Computers* **32**: 396–402.

Orwin JF, Smart CC. 2004. Short-term spatial and temporal patterns of suspended sediment transfer in pro-glacial channels, Small River Glacier, Canada. *Hydrological Processes* **18**: 1521–1542.

Owen LA, Thackray G, Anderson RS, Briner J, Kaufman D, Roe G, Pfeffer W, Yi C. 2009. Integrated research on mountain glaciers: current status, priorities and future prospects. *Geomorphology* **103**: 158–171.

Resource Inventory Standards Committee (RISC). 2009. Manual of British Columbia Hydrometric Standards. *Prepared by the Ministry of Environment Science and Information Branch*. V 1.0. http://www.ilmb.gov.bc.ca/risc [7 June 2011].

Richards G, Moore RD. 2003. Suspended sediment dynamics in a steep, glacier-fed mountain stream, Place Creek, Canada. *Hydrological Processes* **17**: 1733–1753.

Schiefer E, Menounos B, Wheate R. 2007. Recent volume loss of British Columbian glaciers, Canada. *Geophysical Research Letters* **34**: L16503. DOI: 10.1029/2007GL030780

Schiefer E, Slaymaker O, Klinkenberg B. 2001. Physiographically controlled allometry of specific sediment yield in the Canadian Cordillera: a lake sediment-based approach. *Geografiska Annaler* **83**(A): 55–65.

Stott TA, Mount NJ. 2007. Alpine proglacial suspended sediment dynamics in warm and cool ablation seasons: implications for global warming. *Journal of Hydrology* **332**: 259–270.

Stott TA, Nuttall A, Eden N, Smith K, Maxwell D. 2008. Suspended sediment dynamics in the Morteratsch proglacial zone, Bernina Alps, Switzerland. *Geografiska Annaler* **90A**: 299–313.

Stott TA, Owens PN, Forrester, BJ, Lee J. 2009. Suspended sediment fluxes in the Castle Creek Glacier proglacial zone, Cariboo Mountains, British Columbia. *Innovations in Practice* **3**: 49–70.

Swift DA, Nienow PW, Spedding N, Hoey TB. 2002. Geomorphic implications of subglacial drainage configuration: rates of basal sediment evacuation controlled by seasonal drainage system evolution. *Sedimentary Geology* **149**: 5–19.

Syvitski JPM, Milliman JD. 2007. Geology, geography, and humans battle for dominance over the delivery of fluvial sediment to the coastal ocean. *The Journal of Geology* **115**: 1–19.

Tabachnick BG, Fidell LS. 1989. *Using multivariate statistics*, (2nd edn). Harper and Row: New York.

Tennant C, Menounos B, Wheate R, Clague JJ. 2012. Area change of glaciers in the Canadian Rocky Mountains, 1919 to 2006. *The Cryosphere* **6**(6): 1541–1552.

Tunnicliffe JF, Church M. 2011. Scale variation of post-glacial sediment yield in Chilliwack Valley, British Columbia. *Earth Surfaces Processes and Landforms* **36**: 229–243.

Warburton J. 1990. An alpine proglacial fluvial sediment budget. *Geografiska Annaler* **72A**: 261–272.

Water Survey of Canada (WSC). 2012. Hydrometric manual: data computations. Weather and Environmental Monitoring Directorate, issued under the authority of the Assistant Deputy Minister, Meteorological Services of Canada. qSOP-NA037 (Beta Version) 2012-12-17. Water Survey of Canada. http://www.wsc.ec.gc.ca [21 January 2013].

Supporting Information

Additional supporting information may be found in the online version of this article at the publisher's website.